Cerebral Metabolic Differences in Parkinson's and Alzheimer's Diseases Matched for Dementia Severity

Thierry Vander Borght, Satoshi Minoshima, Bruno Giordani, Norman L. Foster, Kirk A. Frey, Stanley Berent, Roger L. Albin, Robert A. Koeppe and David E. Kuhl

Division of Nuclear Medicine and Departments of Internal Medicine, Psychiatry and Neurology, University of Michigan Medical School, and Geriatrics Research, Education and Clinical Center, Department of Veterans' Affairs Medical Center, Ann Arbor, Michigan

Despite controversial clinicopathological distinctions between Parkinson's disease with dementia (PDD) and Alzheimer's disease (AD), similar patterns of metabolic reduction in the posterior brain were reported previously using PET with [^{18}F]fluorodeoxyglucose. The current study was designed to examine more specific regional differences in cerebral glucose metabolism between PDD and AD using accurate and objective brain mapping techniques. **Methods:** This study included nine normal subjects, nine PDD patients and nine AD patients. PDD and AD groups were matched carefully for age, sex and general dementia severity as measured by Mini-Mental State Examination and Clinical Dementia Rating scales. Each subject underwent [^{18}F]fluorodeoxyglucose-PET and neuropsychological testing. After anatomic standardization of PET image sets and stereotactic data extraction, absolute and normalized cerebral metabolic rates were assessed by region of interest and pixel-by-pixel analyses. **Results:** PDD and AD showed global glucose metabolic reduction with similar regional accentuation involving the lateral parietal, lateral temporal and lateral frontal association cortices and posterior cingulate cortex in comparison to normal controls. When comparing between PDD and AD, however, PDD showed greater metabolic reduction in the visual cortex and relatively preserved metabolism in the medial temporal cortex. **Conclusion:** Although a common feature of metabolic abnormalities in the posterior brain exists in PDD and AD, the presence of regional metabolic differences suggests different degrees and combinations of disease specific underlying pathological and neurochemical processes.

Key Words: ; Lewy body disease; Parkinson's disease; Alzheimer's disease; emission computed tomography; fluorine-18-FDG

J Nucl Med 1997; 38:797–802

Dementia occurs in 10%–30% of patients suffering from Parkinson's disease (PD) (*1,2*). Although clinical features are often different between PD with dementia (PDD) and Alzheimer's disease (AD), earlier investigations suspected coexisting AD pathology (senile plaques and neurofibrillary tangles) to be responsible for the dementia occurring in PD patients (*3*). Degeneration of cholinergic neurons in the nucleus basalis of Meynert was found initially in AD (*4*) but subsequently in PDD as well (*5*). Reflecting such pathological similarities, functional similarities also were reported previously using in vivo brain imaging such as PET (*6–8*) and SPECT (*9,10*). These studies commonly found metabolic and blood flow reduction in the posterior part of the brain in PDD and AD.

Other neuropathological studies, however, revealed differences in pathological changes between PDD and AD. AD pathology, such as neurofibrillary tangles, was not found consistently in the neocortex or hippocampus in PDD (*11,12*). Even when AD pathology exists in the cortex of PDD patients, the severity of cortical neuronal involvement (*13*) and regional patterns of AD pathology (*14*) are different between PDD and AD. The degree of neuronal loss in the nucleus basalis and reduction in choline acetyltransferase activity may differ between PDD and AD (*15*). The frequency of the epsilon 4 allele of apolipoprotein E is different between PDD and AD (*16*). These findings suggest the presence of distinct pathological processes that may be involved in PDD, other than the mere coexistence of AD pathology.

The above similarities and dissimilarities between PDD and AD are complicated further by the increasing recognition of Lewy body disease. Lewy bodies are associated historically with PD and found typically in the brainstem nuclei such as the substantia nigra and locus coeruleus in PD (*17*). Similar intracellular inclusions (cortical Lewy bodies) are found also in the neocortex of demented patients with parkinsonism (*18*). The spectrum of Lewy body disease includes idiopathic PD with and without dementia, (pure) diffuse (cortical) Lewy body disease (DLBD) and combined pathology of AD and Lewy bodies. One autopsy study demonstrates coexisting Lewy bodies in the substantia nigra in 23% of AD patients (*19*). In contrast, among PD patients who had dementia antemortem, 29% had similar lesions to AD, 10% had numerous cortical Lewy bodies, 6% had possible vascular origin and 55% has indefinite pathological causes (except "plentiful" cortical Lewy bodies) (*20*). Although an as yet unidentified pathological entity could exist in dementing disorders (*21*), autopsy studies suggest that PDD and AD groups likely represent different populations on a continuum of combinations of several overlapping pathological and neurochemical processes.

We, therefore, hypothesized that cerebral metabolic activity should reveal specific regional differences between PDD and AD reflecting different degrees of underlying pathological processes, in addition to the common features previously observed by functional imaging. To test this hypothesis, an accurate and objective method to analyze PET datasets by means of stereotactic signal localization, surface data extraction and pixel-by-pixel group comparison, including the entire brain (*22*), was used in this study. Age, sex and general dementia severity were matched carefully between PDD and AD groups, so that specific pathological processes could be compared without confounding differences in the severity of the diseases.

MATERIALS AND METHODS

PDD and AD Patients and Normal Control Subjects

PDD and AD groups were carefully matched for age (PDD, 70 ± 6 yr; AD, 69 ± 6 yr), sex (5 men and 4 women in each

Received Apr. 26, 1996; revision accepted Sep. 19, 1996.

For correspondence or reprints contact: Satoshi Minoshima, MD, PhD, Division of Nuclear Medicine, Department of Internal Medicine, The University of Michigan Medical Center, B1G412 University Hospital, Ann Arbor, MI 48109-0028.

group), education (PDD, 10.6 ± 2.5 yr; AD, 11.7 ± 2.1 yr), intellect (Full Scale Intellectual quotient (FSIQ): PDD, 78 ± 12; AD, 78 ± 10) (*23*) and general dementia severity, as measured by the Mini-Mental State Examination (PDD, 18 ± 5; AD, 18 ± 6) (*24*), Clinical Dementia Rating (PDD, 1.2 ± 0.8; AD, 1.3 ± 0.6) (*25*) and Blessed Dementia Rating (PDD, 7.4 ± 6.6; AD, 7.3 ± 3.9) (*26*). The diagnosis of PDD was based on progressive cognitive decline starting at least 6 mo after the Parkinson's symptoms. Such Parkinson's symptoms included two or three of the following: rigidity, bradykinesia or resting tremor for at least 3 mo, and patients had to benefit significantly from dopaminergic agents. Patients were not included if they demonstrated evidence of a supranuclear gaze palsy (except upward gaze), autonomic failure or cerebellar ataxia. One of the PDD patients died during a clinical follow-up period. Autopsy revealed DLBD without concomitant AD pathology, and imaging results from this patient have been reported previously (*27*). The diagnosis of probable AD was based on National Institute of Neurological and Communicative Disorders and Stroke (NINCDS) and Alzheimer's Disease and Related Association (ADRDA) criteria (*28*). Eight PDD patients were on chronic L-DOPA therapy (3,4-dihydroxyphenylalanine and a peripheral decarboxylase inhibitor). Five PDD patients were also taking daily 5–10 mg of deprenyl and one patient was taking 1.25 mg of bromocriptine. None received anticholinergic treatment. AD patients were free from medication known to interact with cognitive functions.

All PDD and AD patients also underwent a battery of neuropsychological tests to evaluate a wide range of functions including memory (Wechsler Memory Scale; passage learning and percent delayed recall), language (Boston Naming Test) (*29*), motor performance (finger tapping and strength of grip) and depression (Hamilton Depression Rating Scale; HDRS) (*30*). Neuropsychometric tests were performed within a few months of the PET study (range, −7 to 4 mo; median, 0). Memory impairment was slightly less severe in PDD (passage learning: PDD, 4.2 ± 1.9, AD, 2.4 ± 1.9, $p = 0.05$; and percent delayed recall, PDD, 43.1 ± 34.2, AD 13.4, ± 21.3, $p = 0.04$), whereas differences in language (Boston Naming Test, PDD, 42.1 ± 13.5; AD, 36.4 ± 13.5), depression scale (HDRS, PDD 13.4 ± 8.3; AD 8.1 ± 5.7) and motor performances (finger tapping, PDD, 32.2 ± 16.3, AD, 42.3 ± 9.1; and strength of grip, PDD, 22.3 ± 12.5; AD, 33.1 ± 11.7) did not show statistically significant differences.

Nine age- and sex-matched controls (68 ± 5 yr; 5 men, 4 women) with no history of neurological, psychiatric or major medical diseases were also included in the study. They had a normal neurologic examination on the day of PET scanning. None met the criteria for dementia as described above.

PET Cerebral Glucose Metabolic Imaging

PET scanning was performed using a Siemens ECAT-931/08-12 scanner, which collects 15 simultaneous slices with a slice-to-slice separation of 6.75 mm. After overnight fasting, the subjects were scanned in a quiet, dimly lit room with their eyes open. Thirty minutes after intravenous administration of 370 MBq (10 mCi) ^{18}F-2-fluoro-2-deoxy-D-glucose, a 30-min emission scan was collected. Images were reconstructed using a Shepp filter with a cutoff frequency of 0.35 cycles per projection element, and attenuation correction was calculated using a standard ellipse fitting method resulting in in-plane image resolution of 7–8 mm full-width-at-the-half-maximum. Quantitative cerebral glucose metabolic rates (CMRglc) were calculated by a standard single scan method using an input function obtained from the radial artery (*31*).

Data Analysis

The quantitative parametric images were transformed into the stereotactic coordinate system using a method described previously (*32*). Both absolute CMRglc and CMRglc normalized to the pons (*33*) were analyzed with stereotactically defined cortical and subcortical volumes of interest (VOIs) and pixel-by-pixel analysis using three-dimensional stereotactic surface projection (3D-SSP) techniques (*22*). Predefined cortical VOIs included the following Brodman areas defined on a standard stereotactic atlas (*34*): lateral frontal association cortex 6, 8, 9, 10, 11, 44, 45, 46 and 47; lateral parietal association cortex 5, 7, 39 and 40; lateral temporal association cortex 21, 22, 37 and 38; lateral occipital association cortex 18 and 19; primary visual cortex 17; primary sensorimotor cortex 1, 2, 3 and 4; posterior cingulate cortex 23 and 31; anterior cingulate cortex 24 and 32; and medial temporal cortex 27, 28, 34 and 35. The whole brain activity was defined as an average of all gray matter structures. An asymmetry index was calculated using VOI values as a percentage ratio of right and left hemispheres ($|\text{right} - \text{left}|/(\text{right} + \text{left})$). Significant regional asymmetry was considered when the index was greater than 10%. Averaged values of right and left hemispheric VOIs were used for statistical analyses. The analysis of variance was first performed to examine group differences among normal controls, AD patients and PDD patients including all cerebral VOIs, except the whole brain value, as repeated measures. Group differences in whole brain and pontine values were assessed also by analysis of variance. When analyzing normalized data, the pons (reference region) was excluded from the analysis. Posthoc univariate F tests with contrasts were performed to test differences between normal controls and AD patients, between normal controls and PDD patients and between AD and PDD patients. A probability of 0.005 was considered to be statistically significant based on multiple comparison adjustment for the multiple regions included in the analysis (Bonferroni correction). Two-sample Student's t statistic tests were used for pixel-by-pixel analysis and to test differences in psychological indices.

RESULTS

Absolute whole brain CMRglc was significantly different among normal controls, AD patients and PDD patients (F ratio = 15.3, $p < 0.00005$). Posthoc analysis demonstrated significant reduction in CMRglc in AD patients (5.47 ± 0.63 mg/100 g/min, mean ± s.d., $p < 0.0001$) and PDD patients (5.52 ± 0.79 mg/100 g/min, $p < 0.0001$) in comparison to that of normal controls (7.22 ± 0.85 mg/100 g/min). Among all cerebral structures included in the VOI analysis, metabolic activity in the pons was most preserved in both AD and PDD (normal, 5.59 ± 0.67; AD, 4.98 ± 0.53, $p > 0.05$; PDD, 5.18 ± 0.67 mg/100 g/min, $p > 0.20$). There was no statistically significant group difference in the pontine activity among three groups (F ratio = 2.26, $p = 0.13$). In this series, only three patients in both AD and PDD showed metabolic asymmetry greater than 10% in the lateral parietal cortices. Normalized regional cerebral glucose metabolism was calculated by averaging both hemispheres and using the pons as a reference region (Table 1, N, AD and PDD). The significant group difference was indicated again in normalized regional glucose metabolic rates (excluding the pons, F = 14.8, $p < 0.0001$).

When considering $p = 0.005$ as a statistical threshold (Bonferroni correction) for the cortical structures, metabolic activity in AD was significantly decreased in the lateral parietal, lateral temporal, lateral frontal and cingulate cortices when compared to normal control subjects (Table 1, AD − N). The greatest reduction was observed in the posterior cingulate cortex. When comparing PDD to normal control subjects, significant metabolic reduction was found in similar structures including lateral parietal, lateral temporal, lateral frontal and cingulate cortices (Table 1, PDD − N). In addition, there was

TABLE 1
Normalized Cerebral Glucose Metabolism in Normal Control Subjects, AD Patients and PDD Patients

	N	AD	PDD	AD − N (%)	PDD − N (%)	AD − PDD (%)
Cortical structures						
Lateral parietal	1.34 ± 0.15	1.01 ± 0.21	1.01 ± 0.22	−25*	−25*	0
Lateral temporal	1.26 ± 0.09	0.96 ± 0.15	1.04 ± 0.13	−24†	−17*	−9
Lateral frontal	1.42 ± 0.14	1.16 ± 0.14	1.11 ± 0.17	−18*	−22*	4
Lateral occipital	1.31 ± 0.10	1.14 ± 0.13	1.04 ± 0.16	−13	−21*	8
Primary visual	1.51 ± 0.13	1.40 ± 0.16	1.17 ± 0.12	−8	−23†	17*
Primary sensorimotor	1.49 ± 0.15	1.30 ± 0.12	1.28 ± 0.14	−12	−14	2
Anterior cingulate	1.20 ± 0.12	0.99 ± 0.13	0.96 ± 0.09	−17*	−20†	3
Posterior cingulate	1.44 ± 0.15	1.05 ± 0.15	1.03 ± 0.09	−27†	−28†	1
Medial Temporal	0.96 ± 0.05	0.85 ± 0.10	0.96 ± 0.06	−12	0	−13*
Subcortical structures						
Thalamus	1.63 ± 0.18	1.42 ± 0.15	1.38 ± 0.11	−13	−16*	3
Striatum	1.46 ± 0.17	1.36 ± 0.16	1.38 ± 0.09	−7	−6	−2
Others						
Cerebellum	1.22 ± 0.04	1.17 ± 0.09	1.13 ± 0.06	−4	−7	3
Whole brain	1.30 ± 0.10	1.10 ± 0.11	1.07 ± 0.11	−15*	−17†	3

*$p < 0.05$, post-hoc univariate F test comparing two groups.
†$p < 0.0005$, post-hoc univariate F test comparing two groups.
Regional cerebral glucose metabolism normalized to the pons (mean ± s.d.) in normal control subjects (N) and AD and PDD patients. AD − N = (AD − N)/N × 100; PDD − N = (PDD − N)/N × 100; AD − PDD = (AD − PDD)/AD × 100.

significant reduction in PDD in the primary visual cortex and mild reduction in the lateral occipital cortex, which were not observed in AD. Metabolic activity in the primary sensorimotor cortex, medial temporal cortex, striatum and cerebellum was relatively preserved in both patient groups. The spatial extent and regional magnitude of cerebral metabolic abnormalities were demonstrated clearly by pixel-by-pixel analysis (Figs. 1 and 2).

When comparing metabolic activities between PDD and AD, metabolic activity in the primary visual cortex in PDD was significantly lower than that in AD (Table 1, AD − PDD, $F = 10.4$, $p < 0.005$). This reduction was also evident in absolute glucose metabolic rates (PDD, 6.03 ± 0.85 versus AD, 6.91 ± 0.68 mg/100 g/min; −29% versus −18% reduction, respectively, relative to normal control subjects). A trend toward greater reduction was found also in the lateral occipital cortex in PDD compared to AD. In contrast, metabolic activity in the medial temporal cortex in PDD was nearly preserved. Although medial temporal metabolism was not decreased significantly in AD compared to normal control subjects (Table 1, AD − N), comparison between PDD and AD showed relative reduction in the medial temporal cortex in AD because of the preservation in PDD (Table 1, AD − PDD, $F = 10.1$, $p < 0.005$). This pattern was also evident in absolute glucose metabolic rates. Absolute metabolic activity in the medial temporal cortex was 4.22 ± 0.55 mg/100 g/min in AD (−22% relative to normal control subjects), which was a milder reduction compared to other cortical areas (e.g., −33% in the lateral parietal cortex and −35% in the posterior cingulate cortex), but medial temporal metabolism was preserved further in PDD (4.97 ± 0.58 mg/100 g/min, −8%). The spatial extent and regional magnitude of cerebral metabolic differences between PDD and AD were demonstrated by pixel-by-pixel analysis (Fig. 3). Areas of metabolic differences clearly delineated the occipital and temporal cortices, and thus, these findings were less likely to be a statistical noise or chance. Metabolic reduction in the visual cortex and medial temporal cortex also was examined individually (Fig. 4). Although metabolic reduction in the visual cortex was somewhat variable in AD and PDD, metabolic preservation in the medial temporal cortex in PDD was invariable compared to normal control subjects.

DISCUSSION

This study revealed that, despite similar hypometabolism in posterior association and lateral frontal cortices, disease-specific regional CMRglc alterations are present in PDD and AD groups that are matched carefully for age, sex and general dementia severity. In comparison to AD, PDD shows a greater metabolic reduction in the primary visual cortex and metabolic preservation in the medial temporal cortex, while AD shows mild reduction in these areas. Metabolic reduction in the posterior cingulate cortex demonstrated in AD only recently (*35*) is present in PDD patients as well. As far as we know, such detailed comparison of regional metabolic activity in carefully matched AD and PDD groups has not been reported previously. The accurate and objective analysis necessary to detect these small metabolic differences has become possible only recently by means of stereotactic anatomic registration (*32*), followed by stereotactically defined VOI analysis and pixel-by-pixel analysis using 3D-SSPs (*22*).

In agreement with previous studies (*6,7,36*), PDD as well as AD patients showed global cerebral glucose hypometabolism compared to age-matched normal control subjects. In addition, regional accentuation of metabolic reduction in the posterior brain (i.e., parietotemporal association cortex) was similar in PDD and AD, consistent with previous observations (*6–8*). Among the posterior regions, the posterior cingulate cortex demonstrated the largest reduction in AD as well as PDD, emphasizing once again the importance of evaluating this region in dementing disorders (*35*). There was a preferential sparing of the primary sensorimotor cortex and subcortical structures in AD and PDD, a result consistent with previous observations in AD (*37*) as well as in PDD (*36*). Glucose metabolism in the pons was reported to be preserved in AD (*33*). Relative preservation of pontine metabolism was found also in PDD in this study.

Extending an initial observation of metabolic reduction in the occipital region in PD and PDD (*38*), greater glucose metabolic

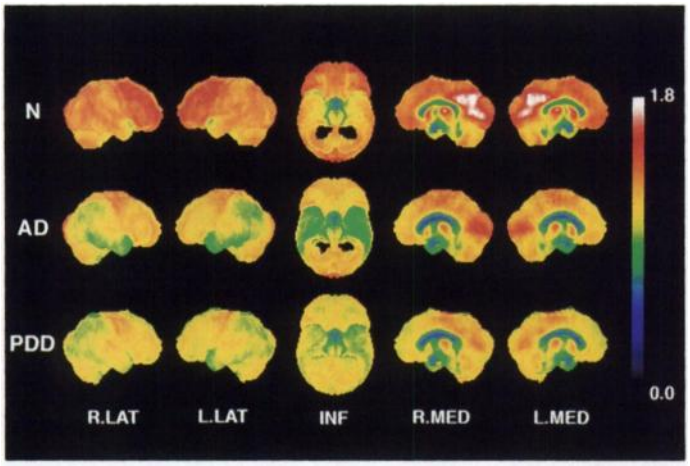

FIGURE 1. 3D-SSPs of normalized CMRglc in normal control subjects (N), AD patients and PDD patients. Each pixel represents a mean metabolic value averaged across nine subjects in each group. Right lateral (R.LAT), left lateral (L.LAT), right medial (R.MED), left medial (L.MED) and inferior (INF) views are shown. Regional hypometabolism in the association cortices is evident.

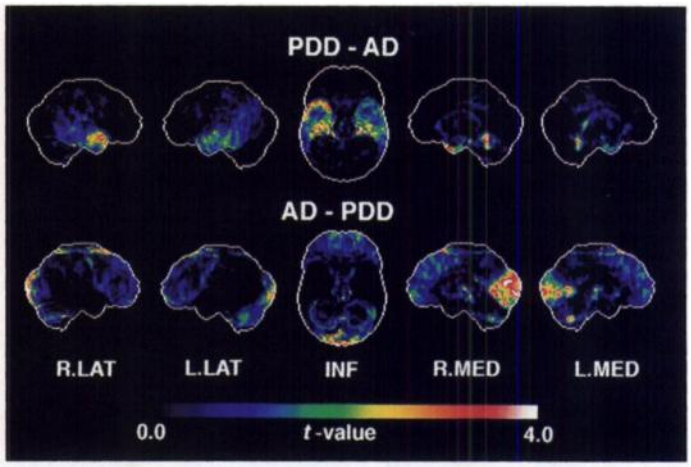

FIGURE 3. Comparison between AD and PDD. 3D-SSP of t statistic maps comparing AD and PDD using normalized CMRglc values. PDD-AD shows those areas in which metabolic reduction in AD is greater than those in PDD. AD − PDD shows those areas in which metabolic reduction in PDD is greater than those in AD. Note relatively greater hypometabolism in the visual cortex in PDD and temporal cortex in AD. Abbreviations are as in Figure 1.

reduction was found in the primary visual cortex in PDD as compared to AD. The lateral occipital cortex also showed significant metabolic reduction. Although room conditions in the PET suite were controlled carefully to maintain the same degree of environmental stimuli, visual attention in each subject, especially in demented patients, was difficult to assess precisely. However, reviewing other published studies, metabolic or blood flow reduction in the occipital cortex in PDD was observed frequently (*10,39*), but was not discussed critically. Similar metabolic reduction was observed also in patients with PD without dementia (*40*) and autopsy-proven DLBD (*27*), suggesting that pathologic and neurochemical abnormalities common to PD, PDD and DLBD may be responsible for the metabolic reduction in the visual cortex. The effects of drug treatment common to these disorders cannot be excluded, but they seem to be less likely since significant treatment effects on cerebral glucose metabolism were not found when studying PD patients with and without chronic dopaminergic medication (*41*). Another possible explanation is that PD or PDD patients reported previously may have included DLBD and that the occipital reduction may be a metabolic feature of DLBD (*27*). However, it is worth noting that abnormalities in the visual system in PD have been characterized previously (*42*). These abnormalities are attributed to dopaminergic systems in the visual pathway (*43*). Retinal dopamine deficiency was indicated by electrophysiological studies (*44*) as well as immunohistochemical studies (*45*). Such primary abnormalities in the visual input from the retina may, at least in part, explain the metabolic reduction in the primary visual cortex in PDD and PD. A flash visual evoked potential study also indicated abnormalities in N1 and N2 latencies in PDD, but not in AD (*46*), consistent with the current metabolic observation.

Metabolic reduction in the medial temporal cortex was mild in AD compared to other cortical areas (e.g., parietal and posterior cingulate cortices). This finding is somewhat puzzling, considering severe degeneration in the medial temporal cortex in AD (*47*), but it is in agreement with the previous observation of mild and variable metabolic reduction demonstrated by a high-resolution PET scanner (*48*). Interestingly, metabolic activity in the medial temporal cortex in PDD was affected even less (Fig. 2), thus medial temporal metabolism in AD appears relatively reduced when compared to PDD (Fig. 3). Such preservation was fairly consistent across PDD subjects (Fig. 4), suggesting that PDD patients included in this study are relatively uniform, at least, for medial temporal abnormalities. Relative metabolic preservation of the medial temporal cortex in PDD has not been reported previously using either metabolic PET or blood flow SPECT. This functional observation, however, seems to be consistent with pathological observations. If

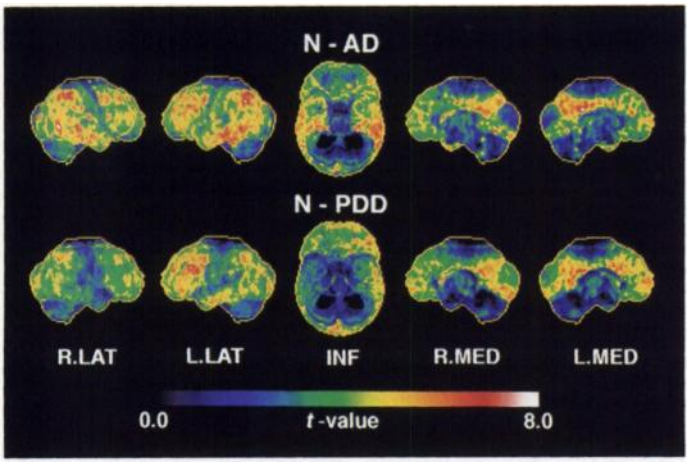

FIGURE 2. Metabolic reduction in AD and PDD. 3D-SSP of t statistic maps comparing AD and PDD to N using normalized CMRglc values. Higher pixel intensity represents more severe metabolic reduction. Note similar CMRglc reduction with relative preservation of the primary sensorimotor cortex and cerebellum in AD and PDD. Metabolic reduction in the medial temporal cortex is minimal in PDD (INF view). Abbreviations are as in Figure 1.

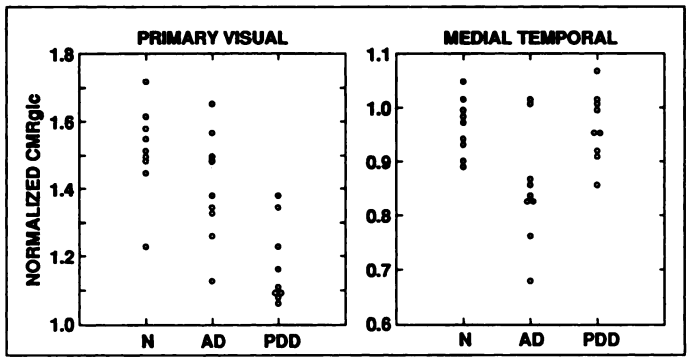

FIGURE 4. Normalized cerebral glucose metabolism of individual subjects in the primary visual cortex and medial temporal cortex in N, AD and PDD patients.

PDD patients in this study have some degree of concomitant AD pathology as discussed previously, such pathological changes seem to be either less frequent or less severe in PDD. For example, when comparing hippocampal and entorhinal AD pathology between AD and PD or PDD, neurofibrillary tangles formation, senile plaque formation and/or reduction in neuronal density were less severe in PD and PDD (*49*). Abnormal Tau proteins indicating the presence of AD-type pathology, were found in PDD, but less severe than AD in the entorhinal cortex, and more prominent in the prefrontal cortex in PDD compared to the temporal cortex (*14*). Alternatively, the observed metabolic difference in the medial temporal cortex may reflect pathological differences between DLBD versus AD. In fact, one of PDD patients in the current study was diagnosed as DLBD by autopsy (*27*). The first metabolic PET study in autopsy-proven DLBD patients revealed relatively preserved metabolic activity in the parahippocampal cortex (*27*), although no comparison with AD was made. AD pathology in the medial temporal cortex in the presence of cortical Lewy bodies is less severe than that in AD pathology alone (*50*). Medial temporal neuronal density is unchanged in DLBD compared with controls (*51*). Synaptic alterations in the hippocampal-entorhinal formation are less severe in DLBD and the Lewy body variant of AD (*52*). Nicotinic binding was severely reduced in the medial temporal cortex in AD, but not in Lewy body dementia (*53*). These previous pathological observations may explain relative metabolic preservation in the medial temporal cortex in PDD observed in this study. When examining neuropsychological test results, PDD showed slightly less severe memory impairment as compared to AD, which coincided with the relative preservation of temporal metabolism. Further investigations, however, are necessary to establish functional significance of the medial temporal pathology in AD and PDD or DLBD.

CONCLUSION

The current study has demonstrated a general similarity in the pattern of metabolic alterations with some specific regional differences in PDD and AD patients who are matched carefully for age, sex and general dementia severity. These findings suggest that PDD and AD may share common features of pathologic and neurochemical alterations along with different degrees and combinations of disease specific underlying pathological and neurochemical processes. Further investigations with a larger number of subjects are warranted to address the neuropsychological significance of such metabolic differences and to compare PET results prospectively with autopsy results.

ACKNOWLEDGMENTS

We thank the PET technologists for their skillful performance in data acquisition, cyclotron operators and chemists for their production of [^{18}F]fluorodeoxyglucose and Vikram Reddy for preparing the manuscript. This study is supported in part by RO1-NS24896 from the National Institutes of Health, DE-FG02-87-ER60561 from the U.S. Department of Energy, P50-AG08671 from the National Institutes of Health (the Michigan Alzheimer's Disease Research Center), P30-AG08808 from the National Institutes of Health (the University of Michigan Claude D. Pepper Older American Independence Center) and the Geriatrics, Research, Education and Clinical Center of the Ann Arbor Veterans' Affairs Medical Center.

REFERENCES

1. Lieberman A, Dziatolowski M, Kupersmith M, et al. Dementia in Parkinson disease. *Ann Neurol* 1979;6:355–359.
2. Brown RG, Marsden CD. How common is dementia in Parkinson's disease? *Lancet* 1984;2:1262–1265.
3. Hakim AM, Mathieson G. Dementia in Parkinson disease: a neuropathologic study. *Neurology* 1979;29:1209–1214.
4. Whitehouse PJ, Price DL, Clark AW, Coyle JT, DeLong MR. Alzheimer disease: evidence for selective loss of cholinergic neurons in the nucleus basalis. *Ann Neurol* 1981;10:122–126.
5. Whitehouse PJ, Hedreen JC, White CL, Price DL. Basal forebrain neurons in the dementia of Parkinson disease. *Ann Neurol* 1983;13:243–248.
6. Kuhl DE, Metter EJ, Riege WH. Patterns of local cerebral glucose utilization determined in Parkinson's disease by the [^{18}F]fluorodeoxyglucose method. *Ann Neurol* 1984;15:419–424.
7. Peppard RF, Martin WR, Carr GD, et al. Cerebral glucose metabolism in Parkinson's disease with and without dementia. *Arch Neurol* 1992;49:1262–1268.
8. Schapiro MB, Pietrini P, Grady CL, et al. Reductions in parietal and temporal cerebral metabolic rates for glucose are not specific for Alzheimer's disease. *J Neurol Neurosurg Psychiatry* 1993;56:859–864.
9. Pizzolato G, Dam M, Borsato N, et al. Technetium-99m-HMPAO SPECT in Parkinson's disease. *J Cereb Blood Flow Metab* 1988;8:S101–S108.
10. Spampinato U, Habert MO, Mas JL, et al. Technetium-99m-HMPAO SPECT and cognitive impairment in Parkinson's disease: a comparison with dementia of the Alzheimer type. *J Neurol Neurosurg Psychiatry* 1991;54:787–792.
11. Mann DM, Yates PO. Pathological basis for neurotransmitter changes in Parkinson's disease. *Neuropathol Appl Neurobiol* 1983;9:3–19.
12. Jellinger K, Riederer P. Dementia in Parkinson's disease, and (pre)senile dementia of Alzheimer type: morphological aspects and changes in the intracerebral MAO activity. *Adv Neurol* 1984;40:199–210.
13. de la Monte SM, Wells SE, Hedley-Whyte T, Growdon JH. Neuropathological distinction between Parkinson's dementia and Parkinson's plus Alzheimer's disease. *Ann Neurol* 1989;26:309–320.
14. Vermersch P, Delacourte A, Javoy-Agid F, Hauw JJ, Agid Y. Dementia in Parkinson's disease: biochemical evidence for cortical involvement using the immunodetection of abnormal Tau proteins. *Ann Neurol* 1993;33:445–450.
15. Candy JM, Perry RH, Perry EK, et al. Pathological changes in the nucleus of Meynert in Alzheimer's and Parkinson's diseases. *J Neurol Sci* 1983;59:277–289.
16. Marder K, Maestre G, Cote L, et al. The apolipoprotein epsilon 4 allele in Parkinson's disease with and without dementia. *Neurology* 1994;44:1330–1331.
17. Lewy FH. Paralysis agitans: I. Pathologische anatomie. In: Lewandowsky M, ed. *Handbuch der Neurologie III*. Berlin: Springer Verlag; 1912:920–933.
18. Kosaka K, Mehraein P. Dementia-Parkinsonism syndrome with numerous Lewy bodies and senile plaques in cerebral cortex. *Arch Psychiatr Nervenkr* 1979;226:241–250.
19. Gibb WR, Mountjoy CQ, Mann DM, Lees AJ. A pathological study of the association between Lewy body disease and Alzheimer's disease. *J Neurol Neurosurg Psychiatry* 1989;52:701–708.
20. Hughes AJ, Daniel SE, Blankson S, Lees AJ. A clinicopathologic study of 100 cases of Parkinson's disease. *Arch Neurol* 1993;50:140–148.
21. Knopman DS, Mastri AR, Frey WHd, Sung JH, Rustan T. Dementia lacking distinctive histologic features: a common non-Alzheimer degenerative dementia. *Neurology* 1990;40:251–256.
22. Minoshima S, Frey KA, Koeppe RA, Foster NL, Kuhl DE. A diagnostic approach in Alzheimer's disease using three-dimensional stereotactic surface projections of fluorine-18-FDG PET. *J Nucl Med* 1995;36:1238–1248.
23. Wechsler D. *Wechsler adult intelligence scale*, revised. New York: Psychological Corporation; 1981.
24. Folstein MF, Folstein SE, McHugh PR. "Mini-mental state." A practical method for grading the cognitive state of patients for the clinician. *J Psychiatr Res* 1975;12:189–198.
25. Gelb DJ, St Laurent RT. Alternative calculation of the global clinical dementia rating. *Alzheimer Dis Assoc Disord* 1993;7:202–211.
26. Blessed G, Tomlinson BE, Roth M. The association between quantitative measures of dementia and of senile change in the cerebral grey matter of elderly subjects. *Br J Psychiatry* 1968;114:797–811.
27. Albin RL, Minoshima S, D'Amato CJ, Frey KA, Kuhl DE, Sima AAF. Fluorodeoxyglucose positron emission tomography in diffuse Lewy body disease. *Neurology* 1996;47:462–466.
28. McKhann G, Drachman D, Folstein M, Katzman R, Price D, Stadlan EM. Clinical diagnosis of Alzheimer's disease: report of the NINCDS-ADRDA Work Group under the auspices of Department of Health and Human Services Task Force on Alzheimer's Disease. *Neurology* 1984;34:939–944.
29. Kaplan E, Goodglass H, Weintraub S. In: *The Boston naming test*, eds., 2nd ed. Boston: Kaplan, Goodglass; 1978.
30. Hamilton M. Development of a rating scale for primary depressive illness. *Br J Soc Clin Psychol* 1967;6:278–296.
31. Hutchins GD, Holden JE, Koeppe RA, Halama JR, Gatley SJ, Nickles RJ. Alternative approach to single-scan estimation of cerebral glucose metabolic rate using glucose analogs, with particular application to ischemia. *J Cereb Blood Flow Metab* 1984;4:35–40.
32. Minoshima S, Koeppe RA, Frey KA, Kuhl DE. Anatomic standardization: linear scaling and nonlinear warping of functional brain images. *J Nucl Med* 1994;35:1528–1537.
33. Minoshima S, Frey KA, Foster NL, Kuhl DE. Preserved pontine glucose metabolism in Alzheimer disease: a reference region for functional brain image (PET) analysis. *J Comput Assist Tomogr* 1995;19:541–547.
34. Talairach J, Tournoux P. *Co-planar stereotaxic atlas of the human brain*. New York: Thieme; 1988.
35. Minoshima S, Foster NL, Kuhl DE. Posterior cingulate cortex in Alzheimer's disease. *Lancet* 1994;344:895.
36. Sasaki M, Ichiya Y, Hosokawa S, et al. Regional cerebral glucose metabolism in

patients with Parkinson's disease with or without dementia. *Ann Nuklearmedizin* 1992;6:241–246.
37. Benson DF, Kuhl DE, Hawkins RA, Phelps ME, Cummings JL, Tsai SY. The fluorodeoxyglucose ^{18}F scan in Alzheimer's disease and multi-infarct dementia. *Arch Neurol* 1983;40:711–714.
38. Kuhl DE, Metter EJ, Benson DF, et al. Similarities of cerebral glucose metabolism in Alzheimer's and Parkinson's dementia. *J Cereb Blood Flow Metab* 1985;5:S169–S170.
39. Liu RS, Lin KN, Wang SJ, et al. Cognition and ^{99m}Tc-HMPAO SPECT in Parkinson's disease. *Nucl Med Commun* 1992;13:744–748.
40. Eberling JL, Richardson BC, Reed BR, Wolfe N, Jagust WJ. Cortical glucose metabolism in Parkinson's disease without dementia. *Neurobiol Aging* 1994;15:329–335.
41. Rougemont D, Baron JC, Collard P, Bustany P, Comar D, Agid Y. Local cerebral glucose utilisation in treated and untreated patients with Parkinson's disease. *J Neurol Neurosurg Psychiatry* 1984;47:824–830.
42. Bodis-Wollner I, Yahr MD. Measurements of visual evoked potentials in Parkinson's disease. *Brain* 1978;101:661–671.
43. Bodis-Wollner I, Yahr MD, Mylin L, Thornton J. Dopaminergic deficiency and delayed visual evoked potentials in humans. *Ann Neurol* 1982;11:478–483.
44. Ikeda H, Head GM, Ellis CJ. Electrophysiological signs of retinal dopamine deficiency in recently diagnosed Parkinson's disease and a follow up study. *Vision Res* 1994;34:2629–2638.
45. Nguyen-Legros J, Harnois C, Di Paolo T, Simon A. The retinal dopamine system in Parkinson's disease. *Clin Vision Sci* 1993;8:1–12.
46. O'Mahony D, Rowan M, Feely J, O'Neill D, Walsh JB, Coakley D. Parkinson's dementia and Alzheimer's dementia: an evoked potential comparison. *Gerontology* 1993;39:228–240.
47. Braak H, Braak E. Neuropathological stageing of Alzheimer-related changes. *Acta Neuropathol (Berl)* 1991;82:239–259.
48. Jagust WJ, Eberling JL, Richardson BC, et al. The cortical topography of temporal lobe hypometabolism in early Alzheimer's disease. *Brain Res* 1993;629:189–198.
49. Ince P, Irving D, MacArthur F, Perry RH. Quantitative neuropathological study of Alzheimer-type pathology in the hippocampus: comparison of senile dementia of Alzheimer type, senile dementia of Lewy body type, Parkinson's disease and non-demented elderly control patients. *J Neurol Sci* 1991;106:142–152.
50. Hansen LA, Masliah E, Quijada-Fawcett S, Rexin D. Entorhinal neurofibrillary tangles in Alzheimer disease with Lewy bodies. *Neurosci Lett* 1991;129:269–272.
51. Lippa CF, Smith TW, Swearer JM. Alzheimer's disease and Lewy body disease: a comparative clinicopathological study. *Ann Neurol* 1994;35:81–88.
52. Wakabayashi K, Honer WG, Masliah E. Synapse alterations in the hippocampal-entorhinal formation in Alzheimer's disease with and without Lewy body disease. *Brain Res* 1994;667:24–32.
53. Katzman R, Galasko D, Saitoh T, Thal LJ, Hansen L. Genetic evidence that the Lewy body variant is indeed a phenotypic variant of Alzheimer's disease. *Brain Cogn* 1995;28:259–265.

Fluorine-18-FDG PET and Iodine-123-IMT SPECT in the Evaluation of Brain Tumors

Wolfgang Weber, Peter Bartenstein, Markus W. Gross, Dieter Kinzel, Hans Daschner, Horst J. Feldmann, Günther Reidel, Sibylle I. Ziegler, Christianto Lumenta, Michael Molls and Markus Schwaiger

Departments of Nuclear Medicine and Radiation Oncology, Klinikum Rechts der Isar; and Department of Neurosurgery Krankenhaus München-Bogenhausen, Technical University of Münich, Münich, Germany

The high glucose utilization of normal gray matter limits the detection of brain tumor tissue by PET using ^{18}F-fluorodeoxyglucose (FDG). The aim of this study was to evaluate whether the examination of amino acid transport with the SPECT tracer ^{123}I-alpha-methyl-L-tyrosine (IMT) allows better identification of tumor tissue than FDG-PET. **Methods:** Nineteen patients (16 with gliomas, 3 with nontumorous lesions) were included in the study. Two independent observers classified PET and SPECT images as positive or negative for tumor tissue and defined the extent of tumor with regions of interest. Tracer uptake of FDG and IMT was quantified by calculating the tumor uptake relative to contralateral gray and white matter. **Results:** SPECT studies were interpreted concordantly in 18 patients (kappa = 0.77) and all tumors were identified by both observers. PET studies were interpreted discordantly in 4 patients (kappa = 0.52) and only 10 tumors were identified by both observers. Interobserver variability in definition of tumor extent was significantly lower in the IMT-SPECT than in the FDG-PET studies ($p = 0.03$). Mean tumor uptake relative to gray and white matter was 1.93 ± 0.42 and 2.25 ± 0.46 for IMT and 0.93 ± 0.32 and 1.61 ± 0.52 for FDG. All tumor uptake ratios were significantly ($p < 0.01$) higher for IMT than FDG, even when only glioblastomas were analyzed. No significant correlation was observed between the various uptake ratios of FDG and IMT. **Conclusion:** Despite the lower resolution and lower sensitivity of SPECT compared with PET, IMT-SPECT was clearly superior to FDG-PET in the detection and delineation of tumor tissue.

Key Words: fluorine-18-FDG; iodine-123-IMT; gliomas

J Nucl Med 1997; 38:802–808

Received Jun. 9, 1996; revision accepted Dec. 20, 1996.

For correspondence or reprints contact: Wolfgang Weber, MD, Department of Nuclear Medicine, Klinikum rechts der Isar, Technical University of Münich, Ismaningerstrasse 22, D-81675 Münich, Germany.

Aggressive neurosurgery, radiotherapy and chemotherapy are the standard of care for most patients with primary brain tumors (*1*). These combined therapeutic strategies can lead to considerable side effects (*2*) and achieve long-term survival only in a small percentage of patients (*3*). Therefore, reliable recognition of viable tumor tissue and measurement of treatment effect are of great importance. Several studies have demonstrated that CT and MRI cannot reliably differentiate viable tumor tissue from tumor-associated edema, postoperative changes or radiation necrosis (*4*). Therefore, imaging methods that are based on specific markers of tumor tissue and metabolism have been proposed as alternatives to these techniques. Since 1982, PET using the glucose analog ^{18}F-fluor-deoxy-D-glucose (FDG) has been applied for noninvasive tumor grading, differentiation of tumor recurrence from radiation necrosis and determination of prognosis (*5–8*). However, the high glucose utilization of gray matter complicates the identification of tumor tissue by FDG-PET (*9–11*). Therefore, difficulties in the visual interpretation of FDG-PET studies and the quantification of FDG uptake were reported (*9,11*). As protein synthesis rate of normal brain tissue is several degrees of magnitude lower than its glucose utilization [about 0.5 nmol/g/min for leucin versus 0.3 μmol/100 g/min for glucose (*12*)], amino acid tracers have been proposed as an alternative to FDG in the metabolic characterization of brain tumors (*13*).

Iodine-123-alpha-methyl-L-tyrosine (IMT) is an amino acid analog initially developed for imaging melanomas and the adrenal medulla (*14*). IMT has a similar affinity to the neutral amino acid carrier at the blood-brain barrier as L-tyrosine but is not further metabolized and not incorporated into proteins (*15,16*). Its uptake in brain tumors can be saturated by natural amino acids, indicating that IMT uptake in these tumors is due